Pressure Spectrum in Homogeneous Turbulence

Toshiyuki Gotoh[1] and Daigen Fukayama[2]

[1]*Department of Systems Engineering, Nagoya Institute of Technology, Showa-ku, Nagoya, 466-8555 Japan*

[2]*Department of Physics, Chuo University, Tokyo, 112-8551 Japan*

(Received 1 May 2000; revised manuscript received 19 October 2000)

The pressure spectrum in homogeneous steady turbulence is studied using direct numerical simulation with resolution up to 1024^3 and the Reynolds number R_λ between 38 and 478. The energy spectrum is found to have a finite inertial range with the Kolmogorov constant $K = 1.65 \pm 0.05$ followed by a bump at large wave numbers. The pressure spectrum in the inertial range is found to be approximately $P(k) = B_p \bar{\epsilon}^{4/3} k^{-7/3}$ with $B_p = 8.0 \pm 0.5$, and followed by a bump of nearly $k^{-5/3}$ at higher wave numbers. Universality and a new scaling of the pressure spectrum are discussed.

DOI: 10.1103/PhysRevLett.86.3775 PACS numbers: 47.27.Ak, 05.20.Jj, 47.27.Gs, 47.27.Jv

The pressure spectrum in an incompressible turbulent flow is defined as $\langle p^2 \rangle = \int_0^\infty P(k)\, dk$. Kolmogorov's theory predicts that

$$P(k) = \bar{\epsilon}^{3/4} \nu^{7/4} \phi(k\eta) \tag{1}$$

$$= B_p \bar{\epsilon}^{4/3} k^{-7/3}, \qquad L^{-1} \ll k \ll \eta^{-1}, \tag{2}$$

where $\phi(x)$ is a nondimensional function, ν is the kinematic viscosity, $\bar{\epsilon}$ is the average rate of energy dissipation per unit mass, L is the integral scale of turbulence, η is the Kolmogorov scale, and B_p is a nondimensional constant of order one [1]. The fluid density is assumed to be unity throughout this paper.

There have been many studies of the pressure spectrum [1–21]. Some of the experiments have shown that $P(k) \propto k^{-7/3}$ [3], or equivalently $D_p = \langle [p(\boldsymbol{x} + \boldsymbol{r}) - p(\boldsymbol{x})]^2 \rangle \propto r^{4/3}$ [13,21]. Others have reported that $r^{4/3}$ is not observed [14]. Recent direct numerical simulations (DNS's) with large scale forcing have found that the pressure spectrum is approximately proportional to $k^{-5/3}$, unlike $k^{-7/3}$, in the wave number range where the energy spectrum scales close to $k^{-5/3}$ [17–19]. Gotoh and Rogallo conjectured that the observed $k^{-5/3}$ scaling for $P(k)$ is a bump, as observed for the energy spectrum, and that $P(k)$ scales as $k^{-7/3}$ in the lower wave number range [19]. There seems to be no agreement about the scaling of the pressure spectrum when compared to the case of the energy spectrum.

We have performed a series of DNS's of incompressible homogeneous isotropic turbulence using a resolution of up to $N = 1024^3$. DNS was designed to generate a wider inertial range and higher Reynolds numbers. The range of the Taylor microscale Reynolds number $R_\lambda = \bar{u}\lambda/\nu$ is between 38 and 478, where $\bar{u}$ is the root mean square of turbulent velocity and λ is the Taylor microscale. The characteristic parameters of DNS are listed in Table I. The code uses the pseudo-Fourier spectrum and fourth order Runge-Kutta-Gill methods. Random forcing, Gaussian and white in time, is applied to the lower wave numbers. A statistically steady state was confirmed by observing the time evolution of the total energy, the total enstrophy, and the skewness of the longitudinal velocity derivative. The statistical averages were taken as the time average over tens of turnover times for lower Reynolds numbers and over a few turnover times for the higher Reynolds numbers. The data of the highest Reynolds number, $R_\lambda = 478$, were obtained as short time average (about 0.34 eddy turnover times) during the passage toward steady state rather than over a statistically steady state. The resolution condition $k_{\max}\eta > 1$ is satisfied for most runs, but that of the case when $R_\lambda = 460$ is slightly less than unity ($k_{\max}\eta = 0.96$). We believe that this does not adversely affect the energy and pressure spectra results in the inertial range. Computations with $R_\lambda \leq 284$ were performed using a Fujitsu VPP700E vector parallel machine with 16 processors at The Institute of Physical and Chemical Research (RIKEN). Simulations using higher R_λ were performed on a Fujitsu VPP5000/56 with 32 processors at the Nagoya University Computation Center.

The energy spectra in Kolmogorov units [multiplied by $(k\eta)^{5/3}$] are shown in Fig. 1. Collapse of curves at various Reynolds numbers is very satisfactory, although the curves

TABLE I. DNS parameters and statistical quantities of runs: $T_{\text{eddy}}^{\text{av}}$ is the length of time average.

R_λ	N	$k_{\max}$	ν	c_f	Forcing range	$T_{\text{eddy}}^{\text{av}}$	E	$\bar{\epsilon}$	L	λ	λ_p	$\eta(\times 10^{-2})$	$F_{\nabla p}$	K	B_p
38	128^3	60	1.50×10^{-2}	1.30	$\sqrt{3} \leq k \leq \sqrt{12}$	22.6	1.99	1.19	0.891	0.501	0.371	4.10	3.62	⋯	⋯
70	256^3	121	4.00×10^{-3}	0.50	$\sqrt{3} \leq k \leq \sqrt{12}$	49.7	1.16	0.457	0.785	0.318	0.256	1.93	5.60	⋯	⋯
125	512^3	241	1.35×10^{-3}	0.50	$\sqrt{3} \leq k \leq \sqrt{12}$	5.52	1.25	0.492	0.744	0.185	0.170	0.841	7.61	⋯	⋯
284	512^3	241	6.00×10^{-4}	0.50	$1 \leq k \leq \sqrt{6}$	3.03	1.96	0.530	1.246	0.149	0.177	0.449	10.4	1.64	⋯
387	1024^3	483	2.80×10^{-4}	0.51	$1 \leq k \leq \sqrt{6}$	1.09	1.81	0.522	1.215	0.0986	0.131	0.255	11.3	1.62	⋯
460	1024^3	483	2.00×10^{-4}	0.51	$1 \leq k \leq \sqrt{6}$	2.14	1.79	0.506	1.150	0.0841	0.119	0.199	11.8	1.64	8.1
478	1024^3	483	2.80×10^{-4}	0.51	$1 \leq k \leq \sqrt{6}$	0.34	2.00	0.419	1.350	0.116	0.167	0.269	11.8	1.71	7.9

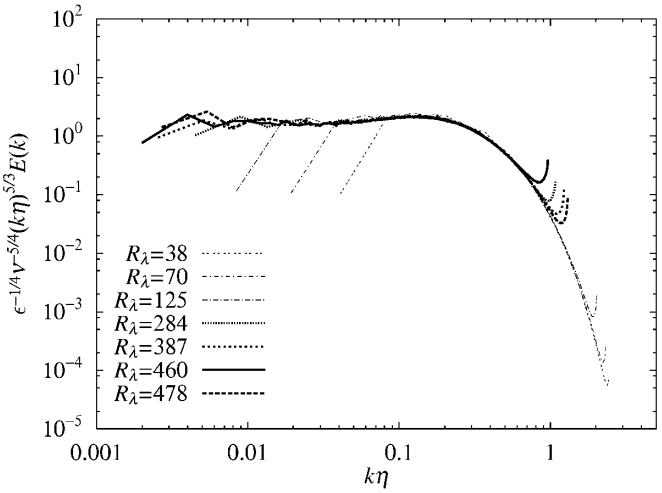

FIG. 1. Scaled energy spectra, $\bar{\epsilon}^{-1/4}\nu^{-5/4}(k\eta)^{5/3}E(k)$. The inertial range is $0.007 \le k\eta \le 0.04$ and $K = 1.65 \pm 0.05$.

with $R_\lambda \ge 284$ have appreciable rise of $E(k)$ near the high wave number boundary. It is clearly seen that the curves with $R_\lambda \ge 284$ have a small but certainly a finite plateau. The Kolmogorov constant K was measured in the range of $0.007 \le k\eta \le 0.04$ in which the average energy transfer flux function $\Pi(k)/\bar{\epsilon}$ is nearly flat and close to unity (figure not shown). The value of K,

$$K = 1.65 \pm 0.05\,, \tag{3}$$

is very close to the value of 1.62 obtained in previous experiments and DNS's [22,23], and to the value of 1.72 obtained using the Lagrangian spectral theory (Lagrangian renormalized approximation) [24,25]. There is a small spectral bump at wave numbers near $k\eta \approx 0.2$, as observed in other DNS's [23] and experiments [26,27].

Figure 2 shows the pressure spectra with the K41 scaling, Eq. (1), multiplied by $(k\eta)^{7/3}$, for various Reynolds numbers. Figure 3 is an enlargement of the higher Reynolds numbers' curves. When $R_\lambda < 300$, the curves do not contain a plateau; however, when $R_\lambda > 300$ and increases, there appears a small plateau between $0.007 \le k\eta \le 0.04$ where the energy spectrum has a $-5/3$ slope. The slope and width of the $R_\lambda = 460$ curve plateau were the same, within the statistical error bar, when the averaging time was doubled. A series of DNS's were also performed with $R_\lambda = 560$, $T_{\text{eddy}}^{\text{av}} = 1.16$, and $k_{\max}\eta \approx 0.76$, which implies that the energy spectrum near the high wave number end is contaminated. Nevertheless, the $k^{7/3}P(k)$ curve contains almost the same plateau as the $R_\lambda = 460$ curve (figure not shown). As a check, the $P(k)$ curve for $R_\lambda = 560$ was compared with that computed from the velocity field, discarding the contaminated Fourier components of $k > 308$. Both pressure spectra were found to be identical in the wave number range of $k\eta < 0.2$. These facts indicate that the plateau of $k^{7/3}P(k)$ certainly exists and is stable.

More careful examination of the $k^{7/3}P(k)$ plateau was undertaken. The $k^{\gamma_p}P(k)$ curve is plotted in Fig. 4 with $\gamma_p = 5/3$, 2.11, 2.28, and 7/3. Between $0.007 \le k\eta \le 0.04$, the plateau has a very small slope. A nearly horizontal curve is produced by compensating with $k^{2.11}$; this exponent was obtained from a least squares fit. The deviation of the exponent from 7/3 is caused by the narrow inertial range and is partly due to the intermittency. Since $P(k)$ is given by $P(k) = F_{LL,LL}(k)$, where $F_{LL,LL}(k)$ is the fourth order moment of the velocity Fourier amplitude [1], the exponent of $P(k) \propto k^{-\gamma_p}$ is evaluated as $\gamma_p = \zeta_4^L + 1$, using the exponent of the fourth order longitudinal velocity structure function $L(r) \propto r^{\zeta_4^L}$. The value of ζ_4^L in the present DNS was $\zeta_4^L \approx 1.28$, which is consistent with the She and Lévêque value [28,29]. This means that the intermittency correction for γ_p is very small, $\Delta\gamma_p = 7/3 - 2.28 \approx 0.05$; therefore, the correction may be neglected, as in the case of the energy spectrum. The deviation $0.22 \approx 7/3 - 2.11$ is larger than the intermittency

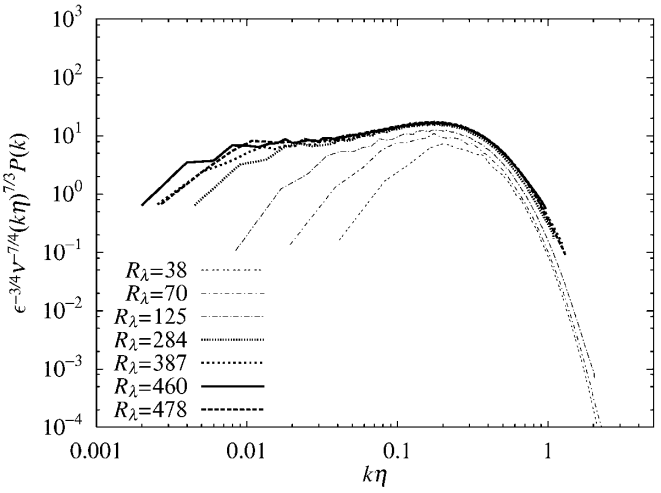

FIG. 2. K41 scaling for the pressure spectra, $\bar{\epsilon}^{-3/4}\nu^{-7/4} \times (k\eta)^{7/3}P(k)$. The inertial range is $0.007 \le k\eta \le 0.04$.

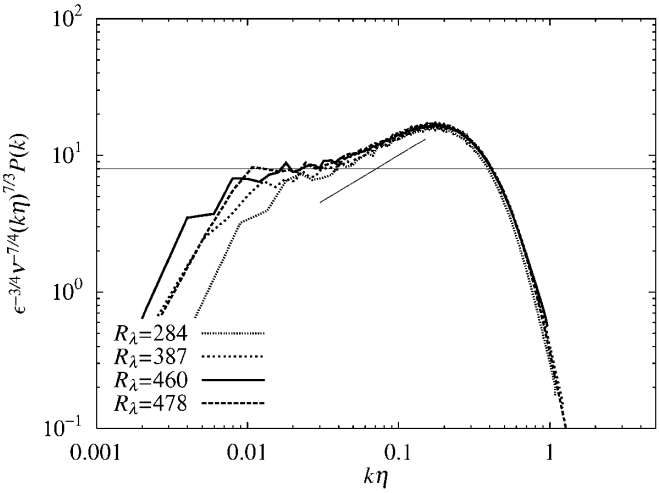

FIG. 3. Closeup of $\bar{\epsilon}^{-3/4}\nu^{-7/4}(k\eta)^{7/3}P(k)$ for higher Reynolds numbers. A short straight line shows the slope of $k^{2/3}$ and a horizontal line indicates $B_p = 8.0$.

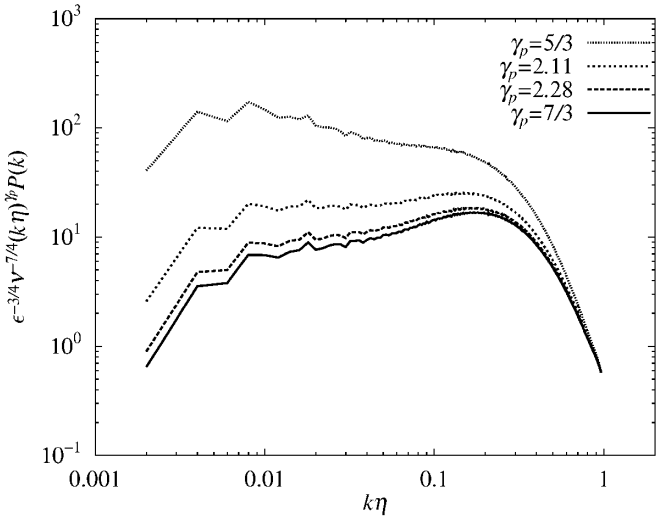

FIG. 4. Comparison of compensated pressure spectrum $\bar{\epsilon}^{-3/4}\nu^{-7/4}(k\eta)^{\gamma_p}P(k)$ at $R_\lambda = 460$. From the uppermost curve, $\gamma_p = 5/3, 2.11, 2.28, 7/3$.

correction, but smaller than the deviation $0.44 \approx 2.11 - 5/3$. From Figs. 2, 3, and 4, the compensation is much more favorable for $k^{7/3}P(k)$ than for $k^{5/3}P(k)$. Therefore, in the inertial range, $P(k) \propto k^{-7/3}$ approximately; $P(k) \propto k^{-5/3}$ does not apply but rather is a part of a bump (see discussion below). When the Reynolds number becomes large enough, it is expected that $P(k)$ tends to Eq. (2) with a possible small intermittency correction to the exponent, $\Delta\gamma_p$, although the approach is very slow.

The curves obtained for $R_\lambda = 387$, 460, and 478 indicate that $P(k)$ approaches the approximate $k^{-7/3}$ spectrum over the range of $0.007 \leq k\eta \leq 0.04$. If $P(k)$ is of the form of Eq. (2), the value B_p is

$$B_p = 8.0 \pm 0.5\,, \tag{4}$$

which is shown in Fig. 3 as a horizontal line. Taking into account the relatively short length of the averaging time, and the finite inertial range, it is reasonable to use a large B_p error bar for the present data.

When the joint Gaussian hypothesis is applied to the fourth order velocity structure functions, B_p is related to the Kolmogorov constant K as [1,3,4,10]

$$B_p = \frac{7}{3}\left(\frac{27}{55}\right)^2 \frac{\Gamma(1/3)^2}{\Gamma(-4/3)} K^2 \approx 1.32K^2. \tag{5}$$

With $K = 1.65$, $B_p = 3.59$, which is smaller than the present DNS value. This is consistent with the fact that $P(k)$ is larger than $P_G(k)$, computed from the Gaussian random velocity field with the same energy spectrum as that of the actual turbulence field [6,7,19]. Pumir suggested that $B_p \approx 7$ using DNS data with $N = 128^3$ at $R_\lambda = 77.5$. Métais and Lesieur computed $P(k) \propto k^{-7/3}$ from a large eddy simulation, with $K = 1.4$ and $B_p = 2.6$. Pullin estimated that $B_p \approx 2.14$–3.65 from Lundgren's stretched spiral vortex model.

There is a bump, with a peak value of about 17, in $P(k)$ near $k\eta = 0.2$ which is more appreciable than that in the energy spectrum. Since the pressure spectrum is related to the fourth order moment of the velocity, the bottleneck phenomenon causes larger amplitude and wider spectral support of the bump [27]. The left part of the bump consists of a finite ramp. For $R_\lambda = 284$, the slope of the ramp is close to 2/3, indicating that $P(k) \propto k^{-5/3}$ (Fig. 3), but the slope gradually decreases as the Reynolds number increases. It is this part which the previous DNS's have observed as $P(k) \propto k^{-5/3}$ [17–19].

The collapse of the $P(k)$ curves for all R_λ's is not as good as the energy spectrum, even in the dissipation range. The collapse of the pressure spectra is improved when the normalized pressure gradient variance, $F_{\nabla p} = \langle(\nabla p)^2\rangle\bar{\epsilon}^{-3/2}\nu^{1/2}$ is included in the scaling for $P(k)$:

$$P(k) = F_{\nabla p}\bar{\epsilon}^{3/4}\nu^{7/4}\phi_1(k\eta)\,, \tag{6}$$

where $\phi_1(x)$ is a nondimensional function [19,20]. Figure 5 presents $P(k)$ using Eq. (6), and clearly shows that the scaling of $P(k)$ in the high wave number range is better than the scaling using Eq. (1). The inset shows the variation of $F_{\nabla p}$ against the Reynolds number. $F_{\nabla p}$ is a monotonically increasing function of R_λ that becomes very weakly dependent on R_λ as R_λ becomes large. It should be noted that although the insensitivity of $F_{\nabla p}$ to R_λ is consistent with Batchelor's Gaussian theory for the pressure, its value is considerably larger than the value corresponding to the Gaussian theory, $F^G_{\nabla p}$ [2,19]. This insensitivity of $F_{\nabla p}$ at large R_λ implies that the collapse of $P(k)$ with $R_\lambda \geq 284$ is little affected by $F_{\nabla p}$. However, there still remains a weak Reynolds number dependence of $P(k)$ in the inertial range, causing the pressure spectrum to be nonuniversal. Close inspection of $P(k)$ in the $k^{-7/3}$ range shows that the factor $F_{\nabla p}$ of Eq. (6) improves the collapse of the curves (Figs. 2 and 5). In this range, $\phi_1(k\eta) = C_p(k\eta)^{-7/3}$ approximately, where C_p is

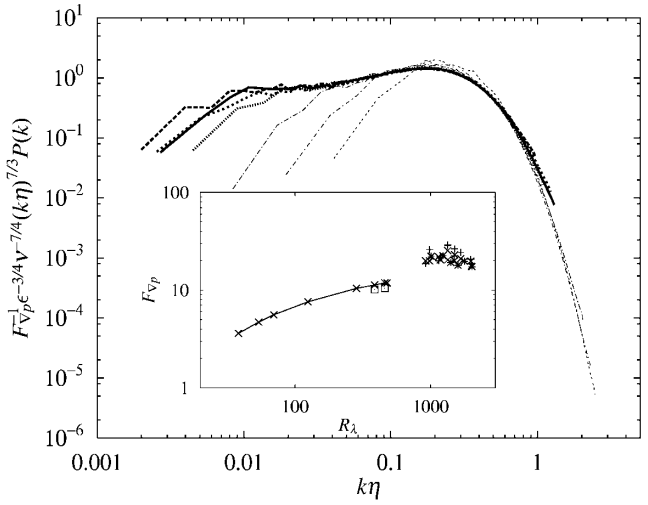

FIG. 5. Scaling of the pressure spectra with the factor $F_{\nabla p}$, $F^{-1}_{\nabla p}\bar{\epsilon}^{-3/4}\nu^{-7/4}(k\eta)^{7/3}P(k)$. The lines are the same as those in Fig. 2. The inset is the variation of $F_{\nabla p}$ against R_λ. Squares are $F_{\nabla p}$ computed by $\lim_{r\to 0}D_p(r)/r^2$, and other symbols are experimental data by Voth *et al.* [16].

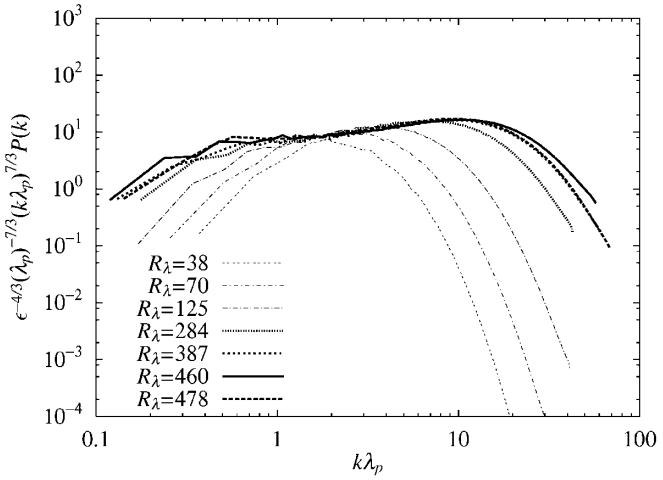

FIG. 6. Scaling of the pressure spectrum in terms of k_p.

a nondimensional constant of the order one. The constant B_p is related as $B_p = F_{\nabla p} C_p$, so that B_p becomes weakly dependent on the Reynolds number, while C_p is not. It is reasonable, in this sense, to regard C_p as a more universal constant than B_p. Using the values of B_p and $F_{\nabla p}$ we obtain

$$C_p = 0.68 \pm 0.04 . \tag{7}$$

The nonuniversality enters the pressure spectrum through $F_{\nabla p}(R_\lambda)$ as a function of R_λ. Therefore, $F_{\nabla p}$ is a key parameter for the second order statistics of pressure at small scales. The Reynolds number dependence of $F_{\nabla p}$ is attributed to the coherent structure of the source term field in the Poisson equation for the pressure [19].

Figure 6 shows that transition of $P(k)$ to the left ramp portion of the bump occurs at $k\eta \approx 0.03$ for $R_\lambda \geq 387$, which corresponds to $k_p \lambda_p \approx 1.5$, and also at 1.8 and 1.6 for $R_\lambda = 460$ and 478, respectively. Here, λ_p is a characteristic length scale for the pressure gradient defined by $\langle (\partial p/\partial x)^2 \rangle = \bar{u}^4/\lambda_p^2$. This is analogous to the Taylor microscale. Thus the crossover scale between the $k^{-7/3}$ and the bump is about $k_p = \lambda_p^{-1}$.

The pressure spectrum at low wave numbers scales as

$$P(k) = \bar{\epsilon}^{4/3} L^{7/3} \phi_2(kL) , \tag{8}$$

where L is the integral scale and $\phi_2(x)$ is a nondimensional function. The curves of $P(k)$ at this range collapse reasonably well into one curve (figure not shown). The scaling of Eq. (6) matches Eq. (8) in the $k^{-7/3}$ range.

The authors acknowledge Professor Antonia and Professor Nakano for their helpful discussions and express their thanks to Nagoya University Computation Center and the Advanced Computing Center at RIKEN for providing the computational resources. This work was supported by a Grant-in-Aid for Scientific Research (C-2 12640118) by The Ministry of Education, Science, Sports and Culture of Japan.

[1] A. S. Monin and A. M. Yaglom, *Statistical Fluid Mechanics* (MIT, Cambridge, MA, 1975), Vol. 2.
[2] G. K. Batchelor, Proc. Cambridge Philos. Soc. **47**, 359 (1951).
[3] W. K. George, P. D. Beuther, and R. E. A. Arndt, J. Fluid Mech. **148**, 155 (1984).
[4] O. Métais and M. Lesieur, J. Fluid Mech. **239**, 157 (1992).
[5] M. Holzer and E. Siggia, Phys. Fluids A **5**, 2525 (1993).
[6] T. Gotoh and R. S. Rogallo, in *Studying Turbulence Using Numerical Simulation Databases, Proceedings of the 1994 Summer Program* (Center for Turbulence Research, Stanford University and NASA Ames Research Center, Stanford, CA, 1994), p. 189.
[7] D. I. Pullin and R. S. Rogallo, in *Studying Turbulence Using Numerical Simulation Databases, Proceedings of the 1994 Summer Program* (Ref. [6]), p. 177.
[8] A. Pumir, Phys. Fluids **6**, 2071 (1994).
[9] M. Nelkin, Adv. Phys. **43**, 143 (1994).
[10] D. I. Pullin, Phys. Fluids **7**, 849 (1995).
[11] R. J. Hill and J. M. Wilczak, J. Fluid Mech. **296**, 247 (1995).
[12] R. J. Hill, Phys. Fluids **8**, 3085 (1996).
[13] M. Ould-Rouis, R. A. Antonia, Y. Zhu, and F. Anselmet, Phys. Rev. Lett. **77**, 2222 (1996).
[14] R. J. Hill and O. N. Boratav, Phys. Rev. E **56**, R2363 (1997).
[15] R. J. Hill and S. T. Thoroddsen, Phys. Rev. E **55**, 1600 (1997).
[16] G. A. Voth, K. Satyanarayan, and E. Bodenschatz, Phys. Fluids **10**, 2268 (1998); A. La Porta, G. A. Voth, A. M. Crawford, J. Alexander, and E. Bodenschatz, Nature (London) **409**, 1017 (2001).
[17] P. Vedula and P. K. Yeung, Phys. Fluids **11**, 1208 (1999).
[18] N. Cao, S. Chen, and G. D. Doolen, Phys. Fluids **11**, 2235 (1999).
[19] T. Gotoh and R. S. Rogallo, J. Fluid Mech. **396**, 257 (1999).
[20] T. Gotoh and K. Nagaya, *Proceedings of IUTAM Symposium on Geometry and Statistics of Turbulence,* edited by T. Kambe, T. Nakano, and T. Miyauchi (Kluwer, Dordrecht, The Netherlands, 1999).
[21] B. R. Pearson and R. A. Antonia (to be published).
[22] K. R. Sreenivasan, Phys. Fluids **7**, 2778 (1995).
[23] P. K. Yeung and Y. Zhou, Phys. Rev. E **56**, 1746 (1997).
[24] Y. Kaneda, J. Fluid Mech. **107**, 131 (1981).
[25] Y. Kaneda, Phys. Fluids **29**, 701 (1986).
[26] S. G. Saddoughi and S. V. Veeravalli, J. Fluid Mech. **268**, 333 (1994).
[27] G. Falkovich, Phys. Fluids **6**, 1411 (1994).
[28] Z. S. She and E. Lévêque, Phys. Rev. Lett. **72**, 336 (1994).
[29] R. Kerr, M. Meneguzzi, and T. Gotoh, Phys. Fluids (to be published).